Thermal Decomposition Kinetics of Wood and Bark and their Torrefied Products

Eszter Barta-Rajnai,[†] Gábor Várhegyi,[,†] Liang Wang,[‡] Øyvind Skreiberg,[‡] Morten Grønli,[§] and Zsuzsanna Czégény[†]*

[†] Institute of Materials and Environmental Chemistry, Research Centre for Natural Sciences, Hungarian Academy of Sciences, PO. Box 286, Budapest, 1519 Hungary

[‡] SINTEF Energy Research, Postboks 4761 Sluppen, NO-7465 Trondheim, Norway

[§] Department of Energy and Process Engineering, Norwegian University of Science and Technology (NTNU), NO-7491 Trondheim, Norway

ABSTRACT. The pyrolysis kinetics of Norway spruce, its bark and their torrefied products was studied. Thermogravimetry (TGA) was employed with linear and stepwise heating programs. Altogether 36 TGA experiments were evaluated simultaneously by the method of least squares. Part of the kinetic parameters could be assumed common for the studied samples without a considerable worsening of the fit quality. This process results in better defined parameters and emphasizes the similarities between the studied materials. Three pseudo-components were assumed. Two of them were described by distributed activation energy models (DAEM), while a simpler kinetics was assumed for the pyrolysis of the

cellulose content of the samples. The pyrolysis kinetics of the wood and the torrefied wood showed remarkable similarities to the bark and torrefied bark, though essential differences were also observed.

1. INTRODUCTION

Torrefaction is a thermal pretreatment of woody and other biomass materials. It increases the energy density, improves hydrophobic behavior, and makes the products easier to be ground.[1-4] Torrefaction is typically conducted at 200–300°C, at atmospheric pressure, in the absence of oxygen. The lignocellulosic biomass is partly decomposed during the torrefaction, releasing condensable liquids and non-condensable gases into the gas phase.[5] Primarily the galactoglucomannan – containing hemicellulose polymers decompose because they are the most reactive polymer structures in biomass.[6,7] The extractives of the biomass also decompose while the cellulose and lignin are moderately impacted during torrefaction, depending on the feedstock composition and the torrefaction temperature.[8]

The present work aims at studying the devotalization kinetics of torrefied products made from wood and bark. The raw materials are also included into the study. Note that bark is a low-priced, abundant by-product of wood processing. Besides, it is a major component of the forest residues and wastes.

The work is part of a broader subject: the pyrolysis kinetics of biomass materials. Due to the complex composition of biomass materials, the conventional linearization techniques of the non-isothermal kinetics are not suitable for the evaluation of the TGA experiments. Therefore the TGA experiments of biomass materials should be evaluated by the non-linear method of least squares, assuming more than one reaction.[9] Biomass fuels and residues contain a wide variety of reactive species. The assumption of a distribution in the reactivity of the decomposing species frequently helps the kinetic evaluation of the pyrolysis of complex organic samples.[10] The distributed activation energy models (DAEM) have been used for biomass pyrolysis kinetics since 1985, when Avni et al. applied a DAEM for the formation of volatiles from lignin.[11] Several variants of DAEMs are known; usually a Gaussian distribution of the

activation energy is employed. The use of DAEM in pyrolysis research was subsequently extended to a wider range of biomasses and materials derived from plants. Due to the complexity of the investigated materials the model was expanded to simultaneous parallel reactions (pseudo-components) that were described by separate DAEMs.[12-15] The increased number of unknown model parameters required the least squares evaluation of larger series of experiments with linear and non-linear temperature programs.[12,16-20]

2. SAMPLES AND METHODS

2.1 Samples. The stem wood and the bark of a representative tree from a Norway spruce (*Picea abies*) forest in South Norway were used. The stem wood was chopped into cubes with size of 1 x 1cm. The bark was chipped into pieces and those with length of around 5-7 cm were used for the torrefaction experiments. The torrefaction experiments were carried out in a tubular reactor in nitrogen atmosphere using a flow rate of 1 L/min. About 80 g samples were treated at temperatures of 225 and 275 °C, using a 60-minute isothermal period. Tables 1 and 2 show the analytical characterization of the wood and bark samples. The mass loss during the torrefaction at 225 and 275 °C is also given in Table 1. The work of Wang et al. contains further analytical data on the samples studied.[21]

Table 1. The Analytical Characteristics of the Raw Materials and the Mass Loss during the Torrefaction

	Wood	Bark
Higher heating value[a]	19.78	20.14
Proximate analysis:[b]		
Volatile matter	81.3	74.6
Ash	0.3	2.4
Fixed carbon	18.4	23.0
Ultimate analysis:[c]		
C	47.38	49.09
H	6.40	6.06
N	0.09	0.45
S	0.01	0.02
O	46.1	44.38
Mass loss during the torrefaction:[d]		
225 °C	8.8	18.5
275 °C	24.3	31.5

[a] MJ/kg, dry basis, measured by bomb calorimeter (IKA Labortechnik C5000). [b] % (m/m), dry basis, according to ASTM standards E872 and D1102. [c] % (m/m), dry ash-free basis. The C, H, N and S were measured by Eurovector EA 3000 CHNS-O Elemental Analyser, while O was calculated by difference. [d] % (m/m), dry basis.

Table 2. Concentration of the Main Ash-Forming Elements in the Raw Materials[a]

	Wood	Bark
Ca	1030	7803
K	272	2011
Si	82	3602
Mg	117	807
S	43	301
Mn	37	771
P	13	407
Zn	18	159

[a] In units of ppm (mg/kg), dry basis. Measured by ICP–OES according to standard CEN/TS 15290:2006. Only the main components are shown (the elements with concentration above 100 ppm in the bark).

For the TGA experiments the untreated and torrefied samples were ground by a cutting mill to <1 mm particle size which was followed by a cryo-grinding to obtain homogenous, representative samples for the TGA experiments. In the treatment the torrefied samples are denoted by the temperature at which they were made preceded by the letter W (wood) or B (bark): B225, B275, W225 and W275. The raw materials are referred to simply as "Bark" and "Wood".

2.2 Experimental Setup and Procedure. The experiments were carried out by a modified Perkin-Elmer TGS-2 thermobalance. Its sensitivity and stability is particularly suitable for experiments with low sample masses, as shown by the repeatability of experiments with 0.2 mg sample mass.[22] In the present work the initial sample masses varied between 0.5 and 4 mg, depending on the temperature programs. The use of the low sample masses served to eliminate the effect of the heat transfer on the reaction rates. This is especially important at higher heating rates, because the reaction rate is roughly proportional with the heating rate. Figure 1 shows the temperature programs employed. Three linear

heating programs were used: 40°C/min, 10°C/min and 2.5°C/min. The corresponding initial sample masses were around 0.5, 2 and 4 mg, respectively. The stepwise heating programs were employed to increase the information content of the series of experiments, as it was explained earlier.[23] Isothermal sections of 20 minutes were employed between 225 and 450°C, as shown in the figure. The heating rate of the non-isothermal sections of these programs was 20°C/min. The Stepwise T(t) denoted by A (represented by red triangles in Figure 1) contained isothermal sections of 225, 275, 325, 375 and 425°C while Stepwise program B was constructed from isothermals at 250, 300, 350, 400 and 450°C. Note that the isothermal sections with temperatures equal to or lower than the torrefaction temperatures are superfluous in the study of the torrefied samples because the low temperature processes had already been completed during the torrefaction. Accordingly they were omitted from the stepwise heating programs of the torrefied samples, as shown in the corresponding figures in the Supporting Information. For the raw materials (wood and bark) three isothermal T(t) programs were also employed. They were composed from a heat-up section (10°C/min), which was also involved into the kinetic evaluation, and a longer isothermal section. In this way 8-8 experiments were carried out on the wood and the bark samples and 5 experiments were carried out on each torrefied samples. The overall number of experiments was 36 (2×8 + 4×5).

The samples were spread on a platinum sample pan of ∅ 6mm. High purity argon was used as purge gas with a gas flow of 140 mL/min.
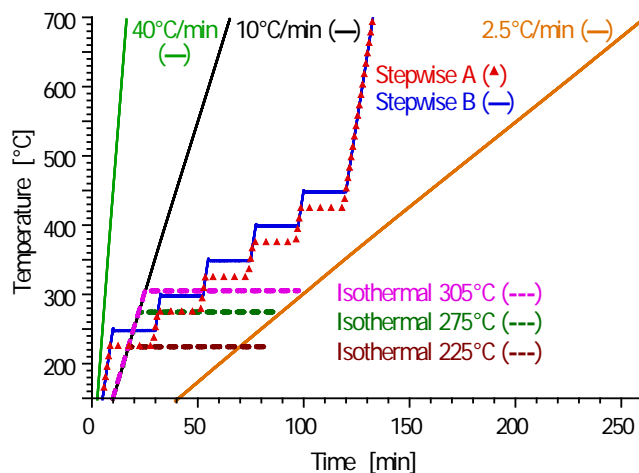
Figure 1. Temperature programs used in the TGA experiments.

2.3. Kinetic Evaluation by the Method of Least Squares and Characterization of the Fit Quality.

Fortran 95 and C++ programs were used for the numerical calculations and for graphics handling, respectively. The employed numerical methods have been described in details earlier.[24] The kinetic evaluation was based on the least squares evaluation of the $-dm^{obs}/dt$ curves, where m^{obs} is the sample mass normalized by the initial dry sample mass. The method used for the determination of $-dm_{obs}/dt$ does not introduce considerable systematic errors into the least squares kinetic evaluation of experimental results.[25] The model was solved numerically along the empirical temperature – time functions. The minimization of the least squares sum was carried out by a direct search method, as described earlier.[24] Such values were searched for the unknown model parameters that minimized the following objective function (*of*):

$$of = \sum_{k=1}^{N_{exper}} \sum_{i=1}^{N_k} \frac{\left[\left(\frac{dm}{dt}\right)_k^{obs}(t_i) - \left(\frac{dm}{dt}\right)_k^{calc}(t_i)\right]^2}{N_k h_k^2} \tag{1}$$

Here N_{exper} is the number of experiments evaluated together. N_k denotes the number of t_i time points on a given curve and m is the sample mass normalized by the initial dry sample mass. The division by h_k^2 serves to counterbalance the high magnitude differences. Traditionally h_k is the highest observed value of the given experiment:

$$h_k = \max \left(\frac{dm}{dt}\right)_k^{obs} \tag{2}$$

The normalization by the highest observed values in the least squares sum assumes implicitly that the relative precision is roughly the same for the different experiments. This assumption has proved to be useful in numerous works on non-isothermal kinetics since 1993.[26]

The obtained fit quality can be characterized separately for each of the experiments evaluated together. For this purpose the relative deviation (*reldev*, %) will be used. The root mean square (rms) difference between the observed and calculated values is expressed as percent of peak maximum. For experiment *k* we get:

$$reldev\,(\%) = 100 \left\{ \sum_{i=1}^{N_k} \frac{\left[\left(\frac{dm}{dt}\right)_k^{obs}(t_i) - \left(\frac{dm}{dt}\right)_k^{calc}(t_i)\right]^2}{N_k h_k^2} \right\}^{0.5} \tag{3}$$

The fit quality for a given group of experiments is characterized by the root mean square of the corresponding relative deviations. In this case a subscript will indicate the number of experiments in the given group, e.g. *reldev*$_{36}$.

3. RESULTS AND DISCUSSION

3.1. Qualitative observations. The pyrolysis of the lignocellulosic materials usually consist of three major and several minor processes. The first major event is the decomposition of the hemicelluloses and part of the extractives[27] which is followed by the cellulose decomposition. The latter forms usually a sharp, well-defined peak in the mass-loss rate curves which is higher than the mass-loss rate belonging to the other phenomena.[28] The cellulose peak on the mass-loss rate curves is followed by a long, flat tailing which corresponds to the lignin pyrolysis (more precisely to the high-temperature part of the lignin pyrolysis) and to the carbonization of the chars formed on lower temperatures.

This well-known picture can clearly be observed in the samples of the present work, too. An obvious exception: the amount of thermally labile species was diminished or completely depleted in the torrefied materials. Figure 2 shows some similarities between the mass-loss rate curves of the untreated samples and their torrefied products. Suitable scaling and an optional shift along the T axis was used to emphasize the similarities, as it is marked in the figure. These observations were used in the set-up of the kinetic model, as outlined in the next sections. Figure 2 clearly reflects that the torrefaction consumes all volatiles species that decompose up to or at the temperature of torrefaction. The thermal decomposition of the cellulose was not changed during the bark torrefaction, as Figure 2a indicates: the peak temperature remained practically the same. The shape and width of the cellulose peak can be checked only at the peak top and right side of the peak, where it is not overlapped by the mass loss of the other components. These sections are practically identical in Figure 2a when the curves are magnified to an equal height, indicating that the torrefaction has not changed the pyrolysis kinetics of the cellulose component. Note that the scaling to equal height in the figure was needed to counterbalance the different amounts of cellulose in the different samples. Another scaling reveals the similarity of the tailing sections in Figure 2b. Note that the tailing section of the mass-loss rate peaks are caused by the lignin decomposition and the slow carbonization of the chars formed at lower temperatures. Figures 2a and 2b also show that the ratio of the cellulose peak and the tailing section decreases during the torrefaction of the bark, indicating that part of the cellulose is lost during the torrefaction.
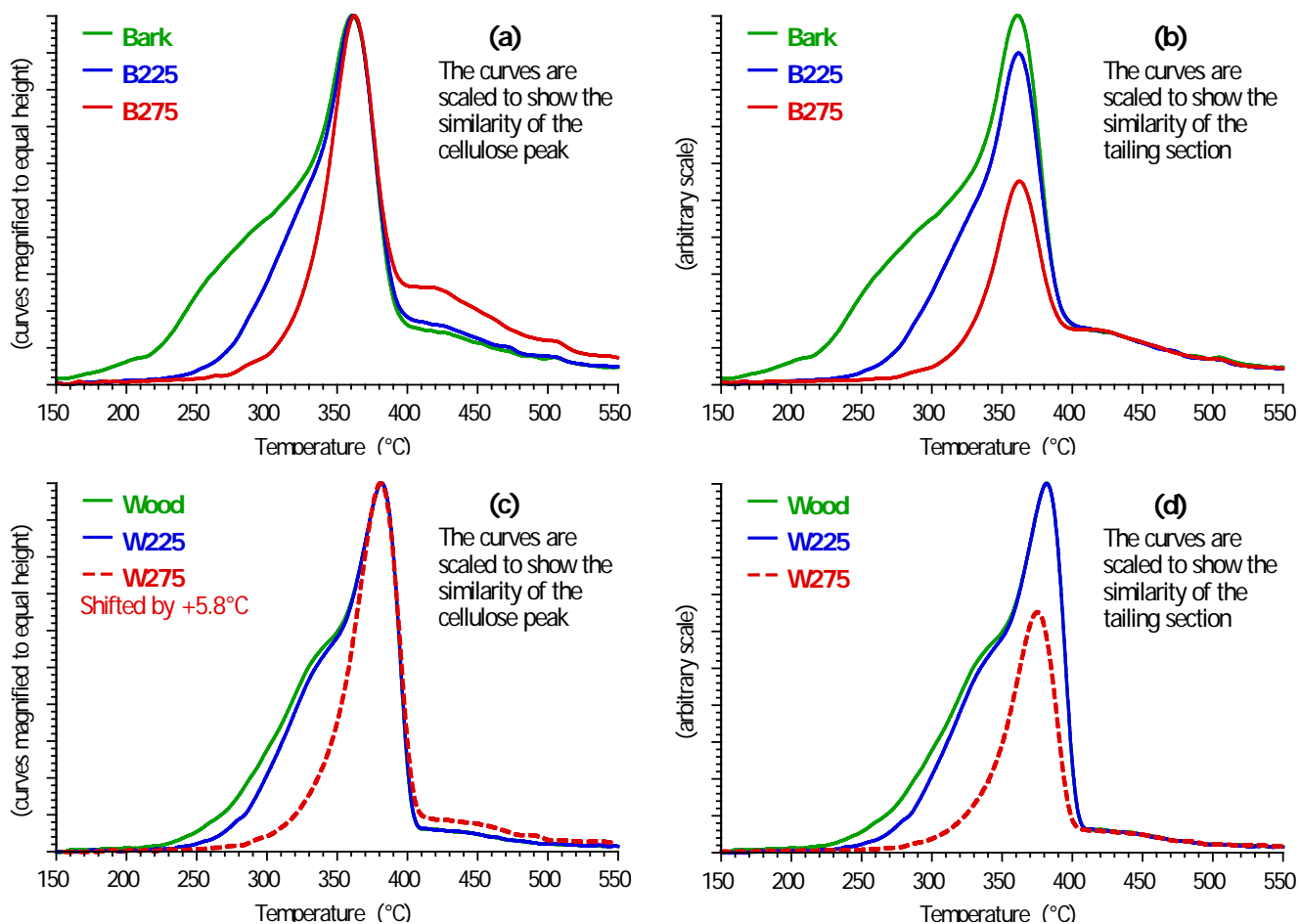
Figure 2. The effects of the torrefaction on the mass-loss rate curves. The scaling on the figure were chosen to emphasize the similarities. The red dashed curve in Figure 2c was shifted up on the T axis by 5.8°C.

The corresponding figures on the wood and wood products (Figures 2c and 2d) are similar to those of the bark and bark products with two exceptions: (i) The cellulose decomposition peak slightly decreased during the 275°C torrefaction. However, when this decrease was compensated by a shift of 5.8°C on the T axis in the plot of Figure 2c, the not-overlaid (i.e. visible) parts of the cellulose peaks revealed the same shape and width for the three samples. (ii) The 225°C torrefaction did not affect the ratio of the cellulose peak height and the height of the tailing section in Figure 2d, indicating that no cellulose loss occurred during the 225°C torrefaction. This was not so in the case of sample B225. As Figure 2b indicates, part

of the cellulose decomposed during the bark torrefaction at 225°C. Note that cellulose pyrolyzed at lower temperatures in the bark samples than in the wood samples; the difference of the corresponding peak temperatures was nearly 20°C at a 10°C/min heating rate. This behavior can probably be due to the catalytic effects of the higher mineral content of the bark.[29]
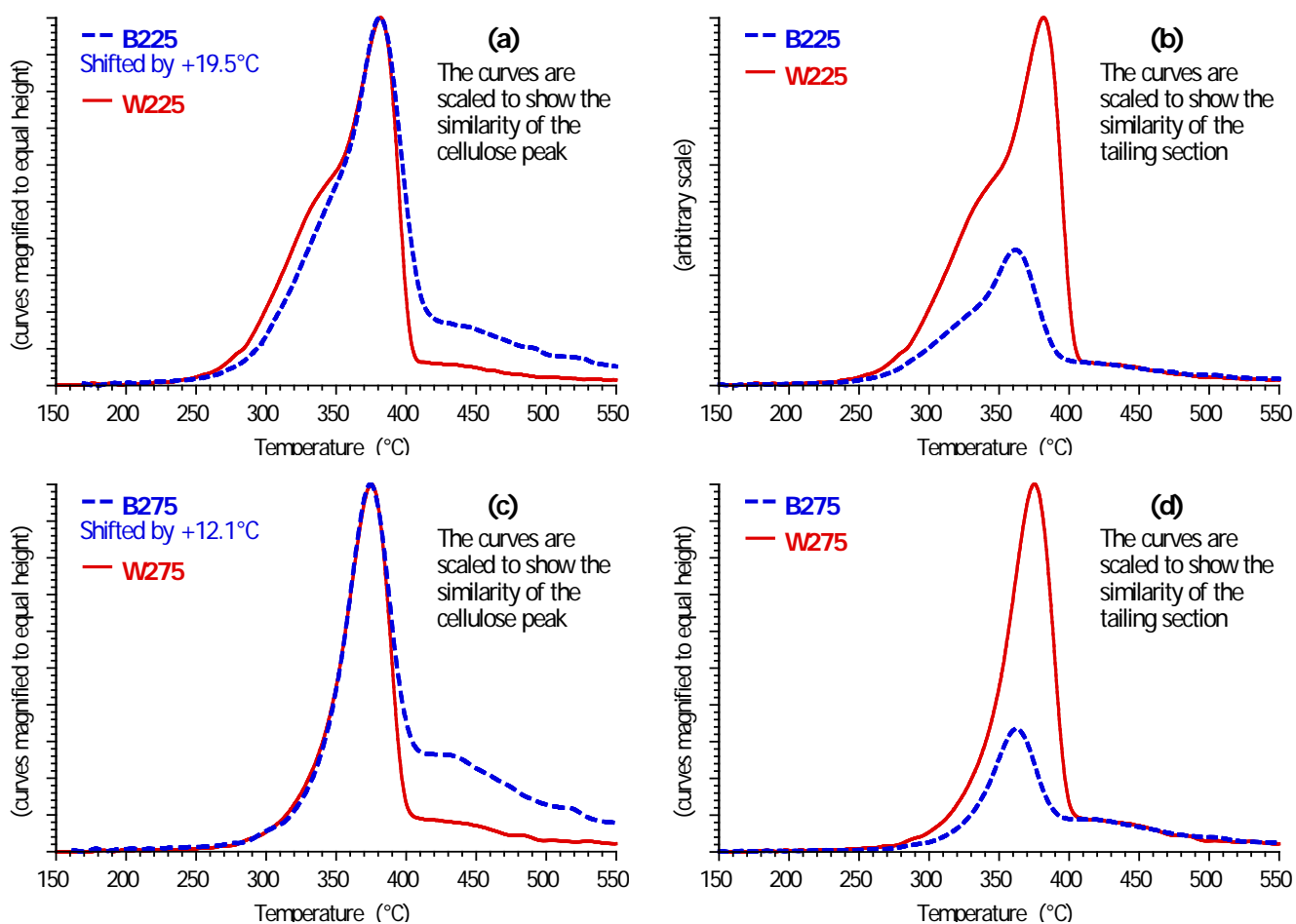

Figure 3. Comparison of the mass-loss rate curves of torrefied bark and torrefied wood curves. The scaling on the figure were chosen to emphasize the similarities. The blue dashed curves in Figures 3a and 3c were shifted up on the T axis, as indicated there.

The behavior of the torrefied bark and wood samples are compared in Figure 3. Here again the observable similarities are emphasized by suitable scaling and by optional shifts along the T axis. Both

the cellulose peaks and the tailing sections exhibits remarkable similarities that were taken into account during the modelling.

3.2. Kinetic model. As mentioned above, the cellulose decomposition forms a sharp, well-defined peak in the mass-loss rate curves of the lignocellulosic materials. This process is usually described by a simple one-step process under the experimental conditions of the thermal analysis, though more complex schemes are also considered, especially when the sample spends long time at temperatures below 300°C.[30] In the present model the cellulose pyrolysis is the second partial reaction, accordingly its reacted fraction (α), activation energy (E) and pre-exponential factor (A) are marked by subscript 2:

$$d\alpha_2/dt = A_2 \exp(-E_2/RT) f(\alpha_2) \tag{4}$$

No justified theories are available about the form of function $f(\alpha_2)$, accordingly two empirical approximations were employed in the work:

$$f(\alpha_2) \cong (1-\alpha_2)^n \tag{5}$$

$$f(\alpha_2) \cong normfactor \, (1-\alpha_2)^n \, (\alpha_2-z) \tag{6}$$

Eq 5 is the widely used n-order kinetics while eq 6 is an empirical formula which can formally describe self-accelerating processes.[31,20] Parameters n and z do not have direct physical meaning; they only serve to determine the shape of $f(\alpha_2)$, as outlined in section 3.6 *normfactor* in eq 6 ensures that the maximum of $f(\alpha_2)$ would be 1, as it is in eq 5. *normfactor* is a simple function of n and z.[31] All evaluations were carried out both with eq 5 and with eq 6. The latter gave better results, as outlined in the next section.

The processes before and after the cellulose decomposition are complex and consist of numerous elementary reactions. They were described by DAEMs, as outlined in the Introduction. In this case the large number of different reacting species are mathematically described by an infinite number of parallel reactions. To avoid an infinitely high number of model parameters, the reactivity differences between the species are described by the distribution of one parameter, the activation energy. To keep the number

of unknown parameters on a low level, a distribution function, usually a Gaussian, is assumed.[10] In the latter case a DAEM has four model parameters: a pre-exponential factor (A), the mean and the scatter of the activation energy distribution (E_0 and σ) and a weight factor (c) that tells what fraction of the overall mass loss is due to the given reaction.

In this way the mass loss rate curves are composed from three partial reactions for samples Wood, Bark, W225 and B225:

$$-dm/dt = c_1\, d\alpha_1/dt + c_2\, d\alpha_2/dt + c_3\, d\alpha_3/dt \tag{7}$$

The number of model parameters is 13 when eq 6 is used: A_1, $E_{0,1}$, σ_1, c_1, A_2, E_2, n, z, c_1, A_3, $E_{0,3}$, σ_3, and c_3.

The first reaction is missing at the samples torrefied at 275°C, as outlined above, in Section 3.1 , hence the number of model parameters is 9 for samples W275 and B275.

3.3. Evaluation by Assuming Common Parameters. Altogether we have 70 model parameters for the 6 samples: 4×13 + 2×9 when eq 6 is employed. 36 experiments were used for their determination. It means less than two unknown parameters for an experiment. Still it turned out that the experiments cannot uniquely define the parameters. Very different sets of parameters can produce good fit between the observed and the simulated data. The problem is illustrated by Figure 4. Figure 4a shows the results at 10°C/min when the five experiments on the bark torrefied at 225°C (B225) was evaluated. Figure 4b displays the results when the 18 experiments on samples Bark, B225 and B275 were evaluated together as outlined below. In Figure 4a the 1st partial curve (represented by blue line) is too wide and too high, while the curve of the cellulose decomposition (red line) is too small. This is unrealistic because a low temperature torrefaction should decrease the amount of hemicelluloses and increase the concentration of cellulose in the remaining product.[21] The problem is caused by the overlap of the partial curves. As the figure shows, only the left-hand side of the blue-colored peak and the right-hand side of the green-colored peak is observable directly. The rest of these curves are hidden by the overlaps and their continuation in

this invisible region is determined by the model. Obviously there are endless possibilities for the construction of the overlapped parts of the partial curves. This is a general problem at overlapping reactions which occur with simpler kinetic equations, too. See e.g. the Appendix of a recent work of Wang et al.[32]
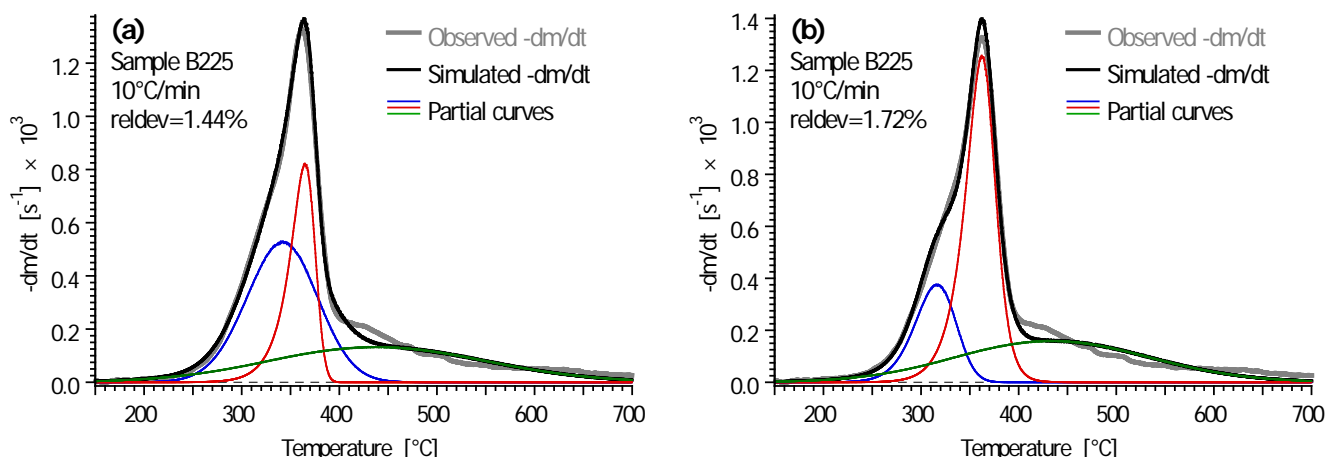

Figure 4. Curve fitting and partial reactions for a selected experiment when **(a)** the five experiments on sample B225 were evaluated; **(b)** the experiments on samples Bark, B225 and B275 were evaluated together, as described in the text.

The problems can be decreased if we restrict the eligible model curves to those which express more or less the observed similarities outlined in section 3.1. This restriction will be carried out by assuming common parameters for different samples. If part of the model parameters is assumed to be common for both samples, two benefits can be achieved:[17-20]

(i) The common parameters help to express the similarities in the kinetic behavior of the samples;

(ii) A given parameter value is based on more experimental information; hence it is less dependent on the various experimental uncertainties.

The base case is Evaluation **1** where none of the parameters was assumed to be common: the experiments of a given samples were evaluated separately from the other samples. In this case the number of experiments evaluated together by eq 1, N_{exper} was 8 for the bark and wood samples and 5 for the rest of the samples. (See Section 2.2 about the experiments available for each sample.) Figure 4a illustrates the results of Evaluation **1**.

Table 3: Fit Quality and the Number of Unknown Parameters in the Evaluations

	Parameters			N_{param} [c]	$\dfrac{N_{param}}{N_{exper}}$ [c]	Fit quality ($reldev_{36}$) [c]
	common for all samples	common for 3 samples [a]	specific for a sample [b]			
1	*none*	*none*	*all*	70 (64)	1.9 (1.8)	1.72 (2.00)
2	*none*	$A_1, A_3,$ $E_{0,1}, E_2, E_{0,3}$ n, z, σ_3	$A_2,$ c_1, c_2, c_3 σ_1	42 (40)	1.2 (1.1)	2.00 (2.20)
3.1	$E_{0,1}, E_2, E_{0,3}$	$A_1, A_3,$ n, z, σ_3	$A_2,$ c_1, c_2, c_3 σ_1	39 (37)	1.1 (1.0)	2.07 (2.27)
3.2	$E_{0,1}, E_2, E_{0,3}$ n, z	$A_1, A_3,$ σ_3	$A_2,$ c_1, c_2, c_3 σ_1	37 (36)	1.0 (1.0)	2.23 (2.37)

[a] In this group the parameters are feedstock-specific: each has one value for the wood and wood products and another for the bark and bark products. [b] Here the parameters have different values for the different samples. [c] The total number of unknowns in the least squares evaluations (N_{param}) and the fit quality ($reldev_{36}$) calculated for all the 36 experiments. N_{param}/N_{exper} is the number of parameter values per experiment. The numbers in the parentheses refer to the same evaluation with n-order cellulose pyrolysis kinetics.

The choosing of the common parameters were based on following considerations:

(i) The c_i parameters in eq 7 depend obviously on the composition of the samples, hence they cannot be considered in the parameter-reduction.

(ii) The amount of the low-temperature volatilization is smaller after a torrefaction at 225°C, and totally missing after a torrefaction at 275°C. The latter fact is expressed so that the first reaction is missing in samples B275 and W275. The decreased low temperature volatilization of samples B225 and S225 was expressed in the model by narrower partial curves, i.e. by smaller σ_1 values for these samples. For this reason σ_1 was allowed to have different values for the different samples during the least squares evaluation. The corresponding E1 and A1 values, however, could be assumed to have a common value for samples Bark and B225 and to have another common value for samples Wood and W225 without a considerable change in *reldev*$_{36}$.

(iii) As Figure 2 indicates, the shape and width of the cellulose peaks do not vary during the torrefaction. However, the cellulose decompose at lower temperature in sample W275 than in samples Wood and W225. The difference is about 6°C at 10°C/min heating rate. The reason for this behavior is not clear because this effect did not occur in the bark products. A moderate change in the peak temperature without a visible change of the shape and width of the peak can be described by different pre-exponential factor values. Accordingly A_2 was allowed to vary from sample to sample.

The above considerations resulted in Evaluation **2** in Table 3. Figure 4b belongs to this evaluation.

In the next step, in Evaluation **3.1**, $E_{0,1}$, E_2 and $E_{0,3}$ were assumed to have identical values in all samples, because this type of restriction proved useful in several earlier works of the authors.[17-20]

As mentioned above, the pyrolysis of the cellulose component was described in two ways: by a two-parameter empirical formula (eq 6) and by *n*-order kinetics. The N_{param} and reldev$_{36}$ values belonging to the latter case are displayed in parentheses in Table 3. Let us have a closer look to the values belonging to the former case (the use of eq 6). Here the constraints of Evaluation **2** decreased the number of

parameters by 28 (from 70 to 42) while $reldev_{36}$ changed by 0.28 (from 1.72 to 2.00). Accordingly the elimination of one unknown parameter value resulted in an increase of 0.010 of $reldev_{36}$ in average. This ratio can be denoted as $\Delta reldev_{36}/\Delta N_{param}$. The next parameter reduction step, from Evaluation **2** to Evaluation **3.1** resulted in higher, but still small changes: $\Delta reldev_{36}/\Delta N_{param}$ was 0.024. In another attempt, Evaluation **3.2**, the n and z parameters of the cellulose decomposition kinetics were also constrained to be identical for the wood and bark-based samples, based on the similarity of the cellulose peaks in Figures 2 and 3. This assumption resulted in somewhat higher $reldev_{36}$: 2.23%. The corresponding $\Delta reldev_{36}/\Delta N_{param}$ is three times higher than in the previous parameter reduction step: it was 0.079.

The use of an n-order kinetics (eq 5) for the cellulose component instead of the two-parameter approximation (eq 6) can also be regarded as a parameter reduction. However, the elimination of parameter z in this way caused much higher $\Delta reldev_{36}/\Delta N_{param}$ ratios than the other parameter reductions employed. It was 0.046 in Evaluation **1**, while the parameter reductions leading to Evaluation **2** resulted in 0.010. Similarly, the $\Delta reldev_{36}/\Delta N_{param}$ was 0.101 when z was eliminated in Evaluation **2**, while the parameter reductions leading to Evaluation **3.1** resulted in a value of 0.024.

Unfortunately the significance of the fit quality changes cannot be judged by the tools of mathematical statistics because the experimental uncertainties of the thermal analysis techniques are not random. Besides, the models are approximate, and approximation errors are obviously not statistical. We regarded Evaluation 3.1 as a reasonable trade-off between the parameter reduction and the fit quality. Its results are shown in details in Section 3.5 and in the Supporting Information.

3.4. About the obtained kinetic parameters. Table 4 shows part of the obtained parameters for Evaluations **1**, **2** and **3.1**. The results of three earlier works with similar models are also presented for a comparison in the bottom of the table. A more complete version of Table 4 containing all parameters for

all evaluations of the present work with more significant figures can be found in the Supporting Information.

The data at the top of the table clearly show that Evaluation **1** (when groups of 5-8 experiments were evaluated separately from the rest of the experiments) did not result in dependable parameters. Especially the kinetic parameters of the third partial process exhibited large, unjustifiable scatterings. $E_{0,3}$, for example, jumps from 195 to 268 kJ/mol for samples Wood and W225, while σ_3 scatters between 24.6 and 39.6. The anomaly shown in Figure 4a is well respected in the c_1 parameter that expresses the amount of mass loss of the first partial process. c_1 is 0.27 for sample Bark and 0.29 for B225 in this evaluation. In reality, however, c_1 should be smaller in B225 than in the untreated bark because the torrefaction decreases the amount of the thermally labile species. These anomalies forced us to decrease the number of the unknown parameter values of the model so that each determined parameter value would be based on more experimental information.

No such problems can be observed among the free (non-common) parameters of Evaluations **2** and **3**. Here the c parameters clearly reflect how the cellulose and lignin is enriched during the torrefaction. The drop of c_2 from sample B225 to sample B275 (from 0.31 to 0.26) expresses the loss of bark cellulose during the torrefaction at 275°C, as it was noted in Section 3.1. The similarity of the $E_{0,3}$ and σ_3 values in the wood and bark groups of the samples indicates the similarities presented in Figure 3.

Table 4: Part of the Obtained Parameters[a] and their Comparison to the Results of Earlier Works

Evaluation	Sample	$E_{0,1}$	E_2	$E_{0,3}$	σ_1	σ_3	c_1	c_2	c_3
1	*(when each sample was evaluated separately)*								
	Wood	179	174	195	8.6	24.6	0.34	0.33	0.17
	W225	157	168	268	4.2	35.7	0.27	0.42	0.15
	W275	–	179	208	–	25.8	–	0.52	0.23
	Bark	179	187	222	13.3	39.6	0.27	0.21	0.22
	B225	184	182	215	9.6	33.1	0.29	0.17	0.22
	B275	–	185	209	–	28.5	–	0.28	0.29
2	*(when two groups of 18 experiments were evaluated)*								
	Wood	177	175	201	8.3	28.4	0.31	0.37	0.18
	W225	177	175	201	5.1	28.4	0.25	0.44	0.16
	W275	–	175	201	–	28.4	–	0.51	0.25
	Bark	180	186	208	15.3	28.7	0.34	0.20	0.16
	B225	180	186	208	4.0	28.7	0.12	0.31	0.24
	B275		186	208	–	28.7	–	0.26	0.32
3.1	*(when the 36 experiments were evaluated together)*								
	Wood	177	176	209	8.5	29.6	0.31	0.37	0.18
	W225	177	176	209	5.1	29.6	0.25	0.43	0.16
	W275	–	176	209	–	29.6	–	0.51	0.25
	Bark	177	176	209	15.2	28.8	0.34	0.20	0.16
	B225	177	176	209	3.9	28.8	0.12	0.32	0.24
	B275	–	176	209	–	28.8	–	0.26	0.32
Earlier results for comparison:									
2013[b]	Norway spruce	169	169	230	8.6	34.2	0.34	0.34	0.17
2012[c]	corncob	180	188	225	3.9	31.3	0.23	0.34	0.20
2011[d]	corn stalk	176	185	195	5.8	36.6	0.11	0.28	0.32

[a] The dimension of $E_{0,1}, E_2, E_{0,3}, \sigma_1$ and σ_3 is kJ/mol. c_1, c_2 and c_3 are dimensionless. See the Supporting Information for the unabridged version of this table. [b] From Table 3 of Tapasvi et al., 2013.[20] [c] From the 7th column in Table 3 of Trninić et al., 2012.[19] [d] From the 1st column in Table 4 of Várhegyi et al., 2011.[18]

The obtained parameters are not far from the results of the previous works with similar models and similar least squares evaluations of series of experiments, as the last three rows indicate in Table 4. The papers cited there were based on more than one sample and several model variants. Those samples and

model variants (evaluation strategies) were selected for comparison which differed the least from the samples and considerations of the present work. For example the work of Trinić at al.[19] studied two corncobs: one of them exhibited an extra low temperature peak while the other was more similar to a usual lignocellulosic material. Obviously the latter was selected for the present comparison. There are some differences between the kinetic parameters of the earlier and the present work in Table 4. However, one should consider here that even the single, well defined mass-loss rate peak of a high purity cellulose resulted in activation energies with a standard deviation of 10 kJ/mol in a round-robin study.[33]

The n and z parameters of the cellulose decomposition are listed in the Supporting Information, in the unabridged version of Table 4. n and z affect the kinetics by defining the $f(\alpha)$ curves, which will be presented and discussed in Section 3.6.

3.5. Fit quality and partial curves. Here the results of Evaluation **3.1** are shown, when 36 experiments were evaluated simultaneously by the method of least squares, as summarized in Table 3. The experiments of samples W225 and B225 are presented in Figures 5 and 6, while the corresponding figures on all experiments together can be found in the Supporting Information.

A good fit can be observed between the observed (gray) and calculated (black) bold lines. The only systematic alteration is at the high temperature reactions of the bark-based samples. Here several lignin pyrolysis reactions take place together with the gradual carbonization of the chars formed at lower temperatures. The employed model mimics only the main course of the resulting mass loss rate without the finer details.
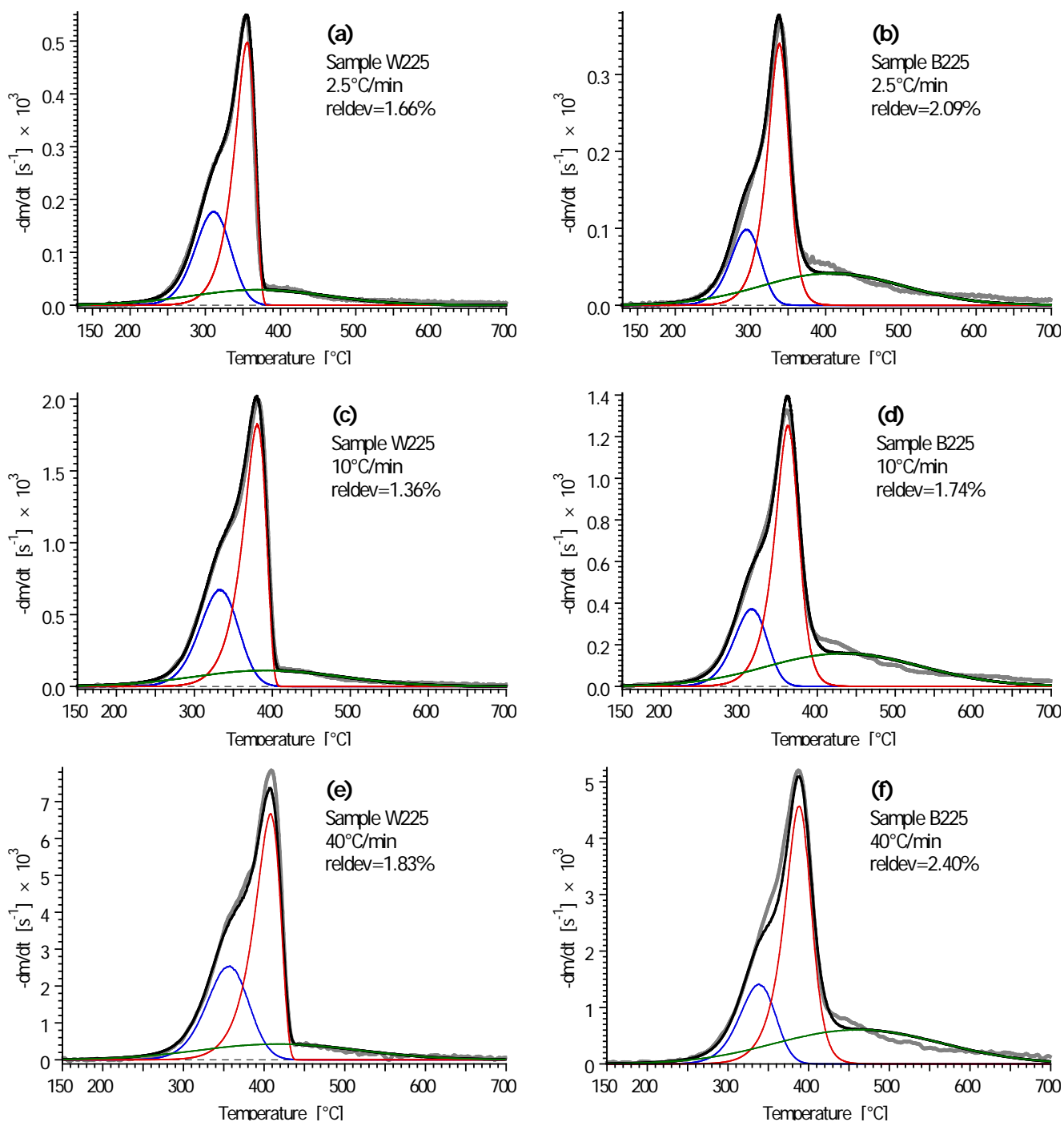
Figure 5. Kinetic curve fitting at linear *T(t)* programs from the results of Evaluation **3.1**. The experiments on the samples torrefied at 225°C are shown. Notation: thick gray line, *-dm^{obs}/dt*; thick black line, *-dm^{calc}/dt*; blue, red and green lines, mass loss rate curves of the pseudo-components. (See Figure 6 and the Supporting Information for more figures from this evaluation.)
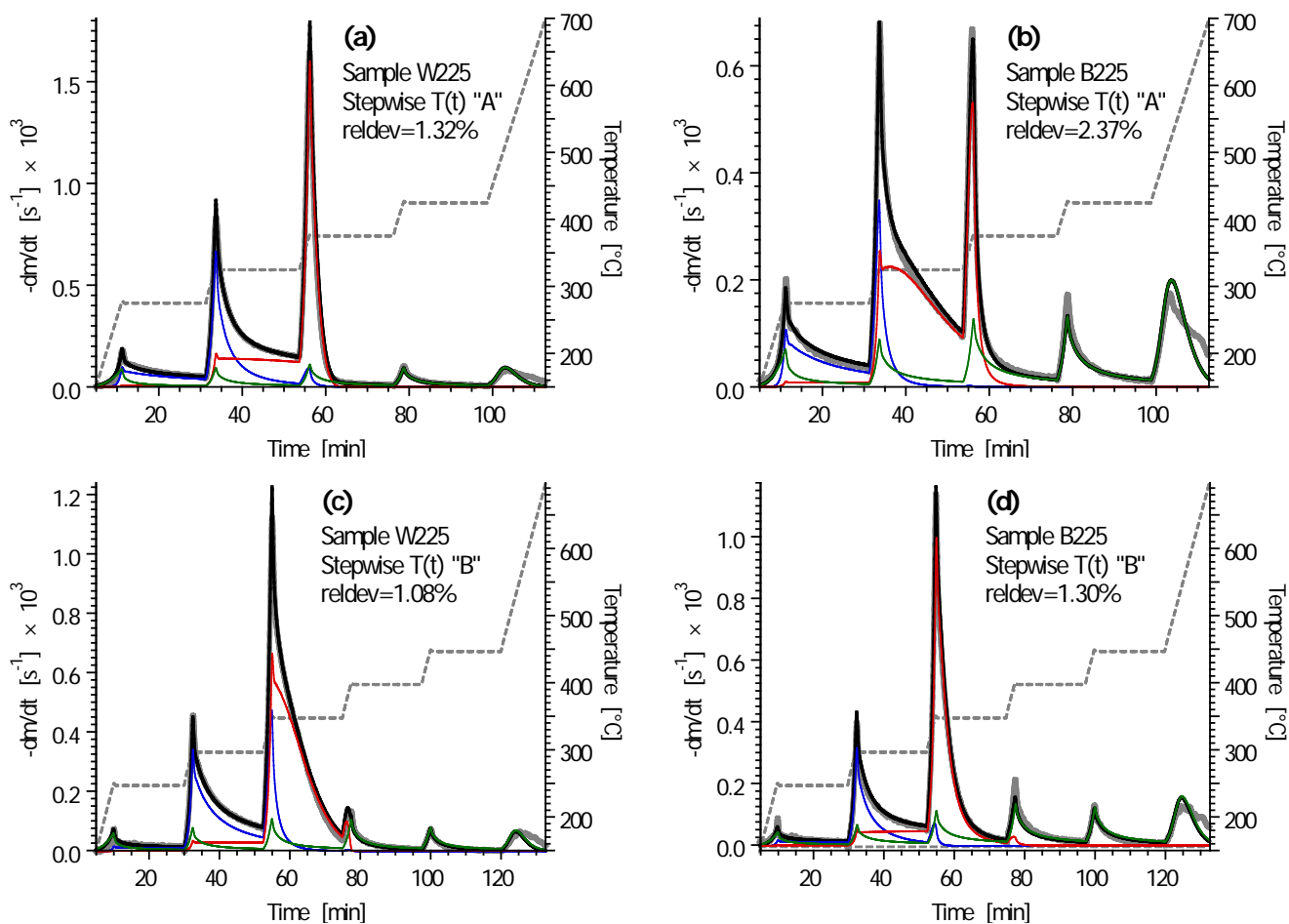
Figure 6. Kinetic curve fitting at stepwise *T(t)* programs from the results of Evaluation **3.1**. The experiments on the samples torrefied at 225°C are shown. Notation: dashed gray line, *T(t)*; thick gray line, *-dm^{obs}/dt*; thick black line, *-dm^{calc}/dt*; blue, red and green lines, mass loss rate curves of the pseudo-components. (See Figure 5 and the Supporting Information for more figures from this evaluation.)

It may be interesting to observe in Figure 5 that the first (blue) partial curve prolongs to relatively high temperatures for sample W225. In reality the thermal decomposition of the hemicelluloses terminates around 350°C at 10°C/min,[34] and around 400°C at 50°C/min.[35] (The latter heating rate is the closest match in the literature to the 40°C/min of the present work.) The same phenomena occurs in the figures of the untreated wood and bark samples, too, as shown in the Supporting Information. This fact indicates that the first pseudo-component describes parts of the lignin-decomposition, as well (i.e. it includes some

pyrolyzing species that belong to the lignin). It is difficult to create an exact border between the first and the third pseudo-components because they strongly overlap each other. On the other hand, the low-temperature section of the third (green) partial curve is not unrealistic because the thermal decomposition of the lignin starts at low temperatures and occurs in a particularly wide temperature domain.[36,37]

3.6. Pyrolysis kinetics of the cellulose component. The cellulose decomposition was described by eq 4 where $f(\alpha_2)$ was approximated by equations 5 and 6. Figure 7a shows the shape of the $f(\alpha_2)$ functions obtained during the simultaneous evaluation of 36 experiments (Evaluations **3.1** and **3.2**). The dashed lines show the *n*-order approximation (eq 5) while the solid lines represent the results obtained by eq 6. The curves differ by concavity: the solid lines are more concave. The solid blue lines, obtained for the bark and the torrefied bark samples, exhibit even some self-acceleration. When a common approximation was searched for all samples by eq 6 the curve represented by black circles was obtained, which is close to the $f(\alpha_2)$ of the wood and torrefied wood (red solid line).

Figure 7b shows the corresponding mass-loss rate peaks obtained for samples B225 and W225 at 10°C/min heating rate. Here the variants obtained for W225 (red color curves) are near to each other, while characteristic, but moderate differences appear for sample B225 (blue curves).
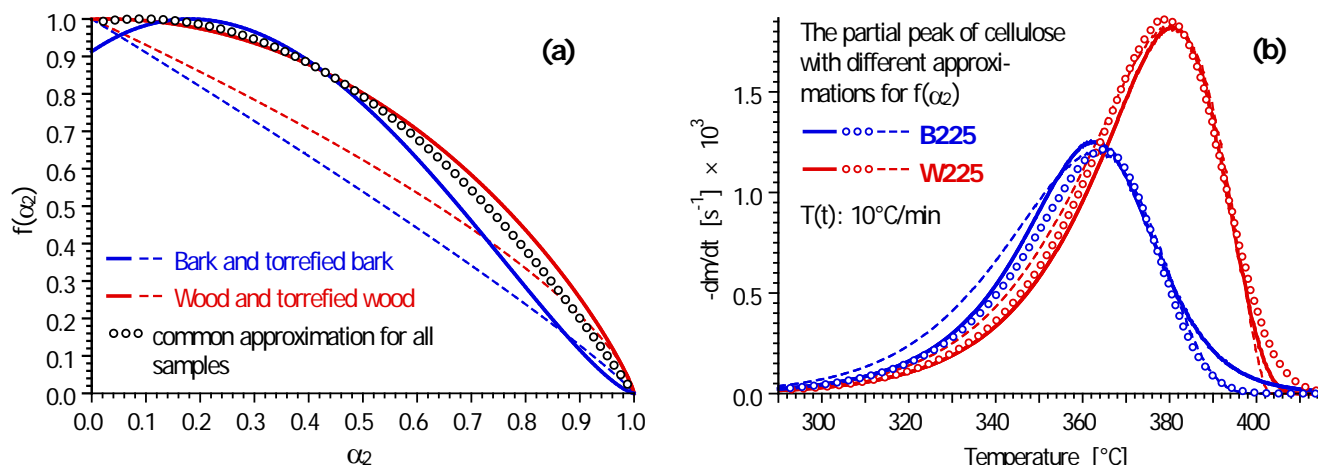
Figure 7. Kinetics of the cellulose pyrolysis in Evaluations **3.1** and **3.2**: The shape of the employed $f(\alpha_2)$ approximations **(a)**; and simulated mass loss rate peaks for Samples B225 and W225 at 10°C/min **(b)**. Notation: *n*-order kinetics, dashed lines; eq 6, solid lines; a common approximation for all samples by eq 6, circles. Colors: as indicated in the figure.

4. CONCLUSIONS

(1) The thermal decomposition of spruce wood, spruce bark and their torrefied products were studied at slow heating programs, under well-defined conditions. Altogether 36 TGA experiments were evaluated by the method of least squares to obtain dependable information and modelling on the kinetics. Highly different temperature programs were selected to increase the information content of the series of experiments.

(2) The bark and torrefied bark samples were included into the studies because bark is a low-priced feedstock and it is an important part of the forest residues. The torrefaction eliminated the prominent low-temperature devolatilization part of the bark. Its cellulose content pyrolyzed at lower temperature than that of wood, which explains why a part of the bark cellulose was lost at the torrefaction at 225°C.

(3) Despite the above differences, considerable similarities were found between the pyrolysis of the bark and torrefied barks and the wood and torrefied woods.

(4) The decomposition of the non-cellulosic parts of the biomass was described by two reactions assuming distributed activation energy models. The first was associated mainly with the hemicelluloses, though extended to other reactive species, as well. This pseudo-component was missing in the samples torrefied at 275°C, because the hemicelluloses and other less-reactive species were decomposed during the torrefaction. The second DAEM corresponded mainly to the lignin pyrolysis, and it also included the mass loss due to the slow carbonization of the chars. The cellulosic component was described in two ways: by *n*-order kinetics and by a two-parameter approximation. The latter gave more favorable results. The complexity of the applied model reflects the complexity of the studied materials.

(5) The model contained 70 parameters altogether for the description of the 36 experiments on six samples. Hence we had less than two unknown parameter values per experiment. Nevertheless, the parameters were not defined well because the overlapping parts of the partial curves can be described in endless ways. To solve the problem, the number of parameters were reduced by appropriate assumptions. In this way the number of unknown parameter values per experiment decreased from 1.9 to 1.1 while the relative deviation between the observed and simulated data was increased by a factor of 1.2.

(6) The assumptions used to decrease the number of unknown parameter values were based on the observed similarities and expressed them in a mathematical form. After the parameter-reductions the determination of a given parameter value was based on more experimental information.

ASSOCIATED CONTENT

Supporting Information

A detailed table on the kinetic parameters obtained for the various assumptions, and figures showing the partial curves and fit quality for all evaluated experiments in Evaluation **3.1**. This material is available free of charge via the Internet at http://pubs.acs.org.

AUTHOR INFORMATION

Corresponding Author

* To whom correspondence should be addressed. E-mail: varhegyi.gabor@t-online.hu, Tel. +36 1 2461894.

NOMENCLATURE

α = reacted fraction of a component or pseudo-component (dimensionless)

σ = width parameter (variance) of Gaussian distribution (kJ/mol)

A = pre-exponential factor (s^{-1})

E = activation energy (kJ/mol) or the mean of an activation energy distribution (kJ/mol)

f = empirical function (eq 4) expressing the change of the reactivity as the reactions proceed (dimensionless)

h_k = height of an experimental $-dm/dt$ curve (s^{-1})

m = the mass of the sample normalized by the initial dry sample mass (dimensionless)

n = reaction order (dimensionless)

of = objective function minimized in the least squares evaluation (dimensionless)

N_{exper} = number of experiments evaluated together by the method of least squares

N_k = number of evaluated data on the kth experimental curve

N_{param} = the total number of unknown parameters in a given model variant

R = gas constant (8.3143×10^{-3} kJ mol^{-1} K^{-1})

reldev = the deviation between the observed and calculated data expressed as per cent of the corresponding peak height

reldev$_{36}$ = root mean square of the *reldev* values of 36 experiments

t = time (s)

T = temperature (°C, K)

z = formal parameter in eq 6 (dimensionless)

Subscripts:

i = digitized point on an experimental curve

j = pseudo-component

k = experiment

REFERENCES

1.   van der Stelt, M. J. C.; Gerhauser, H.; Kiel, J. H. A.; Ptasinski, K. J. Biomass upgrading by torrefaction for the production of biofuels: A review. *Biomass Bioenergy* **2011**, *35*, 3748-3762.

2.   Chew, J. J.; Doshi, V. Recent advances in biomass pretreatment – Torrefaction fundamentals and technology. *Renew. Sustain. Energy Rev.* **2011,** 15, (8), 4212-4222.

3.   Tapasvi, D.; Khalil, R. A.; Skreiberg, Ø.; Tran, K.-Q.; Gronli, M. G. Torrefaction of Norwegian birch and spruce – An experimental study using macro-TGA. *Energy Fuels* **2012**, *26*, 5232−5240.

4.   Bach, Q-V; Skreiberg. Ø. Upgrading biomass fuels via wet torrefaction: A review and comparison with dry torrefaction. *Renew. Sust. Energy Rev.* **2016**, *56*, 665-677.

5.   Prins, M. J.; Ptasinski, K. J.; Janssen, F. J. J. G. Torrefaction of wood. *J. Anal. Appl. Pyrolysis* **2006,** *77*, 35-40.

6.   Rousset, P.; Davrieux, F.; Macedo, L.; Perré, P. Characterisation of the torrefaction of beech wood using NIRS: Combined effects of temperature and duration. *Biomass Bioenergy* **2011,** 35, 1219-1226.

7.   Melkior, T.; Jacob, S.; Gerbaud, G.; Hediger, S.; Le Pape, L.; Bonnefois, L.; Bardet, M. NMR analysis of the transformation of wood constituents by torrefaction. *Fuel* **2012,** 92, (1), 271-280.

8.   Chen, W.-H.; Kuo, P.-C., Torrefaction and co-torrefaction characterization of hemicellulose, cellulose and lignin as well as torrefaction of some basic constituents in biomass. *Energy* **2011,** 36, (2), 803-811.

9.   Várhegyi, G. From "sirups" to biocarbons. A 30 year cooperation research for better biomass utilization with Michael J. Antal, Jr. *Energy Fuels* **2016**, *30*, 7887-7895.

10.   Solomon, P. R.; Serio, M. A.; Suuberg, E. M. Coal pyrolysis: experiments, kinetic rates and mechanisms. *Prog. Energy Combust. Sci.* **1992**, *18*, 133-220.

11.   Avni, E.; Coughlin, R. W.; Solomon P. R., King H. H. Mathematical modelling of lignin pyrolysis. *Fuel* **1985**, *64* 1495-1501.

12.   Várhegyi, G.; Szabó, P.; Antal, M. J., Jr. Kinetics of charcoal devolatilization. *Energy Fuels* **2002**, *16*, 724-731.

13.   de Jong, W; Pirone, A; Wojtowicz, M. A. Pyrolysis of Miscanthus Giganteus and wood pellets: TG-FTIR analysis and reaction kinetics. *Fuel,* **2003**, *82*, 1139-1147.

14.   Wójtowicz, M. A.; Bassilakis, R.; Smith, W. W.; Chen, Y.; Carangelo, R. M. Modeling the evolution of volatile species during tobacco pyrolysis. *J. Anal. Appl. Pyrolysis*, **2003**, *66*, 235-261.

15.   Yi, S-C.; Hajaligol, M. R. Product distribution from the pyrolysis modeling of tobacco particles. *J. Anal. Appl. Pyrolysis*, **2003**, *66*, 217-234.

16.   Becidan, M.; Várhegyi, G.; Hustad, J. E.; Skreiberg, Ø. Thermal decomposition of biomass wastes. A kinetic study. *Ind. Eng. Chem. Res.* **2007**, *46*, 2428-2437.

17.   Várhegyi, G.; Czégény, Zs.; Jakab, E.; McAdam, K.; Liu, C. Tobacco pyrolysis. Kinetic evaluation of thermogravimetric – mass spectrometric experiments. *J. Anal. Appl. Pyrolysis* **2009**, *86*, 310-322.

18.   Várhegyi, G.; Bobály, B.; Jakab, E.; Chen, H. Thermogravimetric study of biomass pyrolysis kinetics. A distributed activation energy model with prediction tests. *Energy Fuels,* **2011**, *25,* 24-32.

19.   Trninić, M.; Wang, L.; Várhegyi, G.; Grønli, M.; Skreiberg, Ø. Kinetics of corncob pyrolysis. *Energy Fuels,* **2012**, *26, 2005-2013.*

20.   Tapasvi, D.;   Khalil, R.; Várhegyi, G.;   Tran, K.-Q.; Grønli, M.; Skreiberg, Ø. Thermal decomposition kinetics of woods with an emphasis on torrefaction. *Energy Fuels* **2013**, *27,* 6134-6145.

21.   Wang, L.; Barta-Rajnai, E.; Skreiberg, Ø.; Khalil, R.; Czégény, Zs.; Jakab, E.; Barta, Zs.; Grønli, M.; Impact of torrefaction on woody biomass properties. *Energy Procedia* **2016**, *in Press*.

22.   Mészáros, E.; Várhegyi, G.; Jakab, E.; Marosvölgyi, B. Thermogravimetric and reaction kinetic analysis of biomass samples from an energy plantation. *Energy Fuels* **2004**, *18*, 497-507.

23.   Várhegyi, G.: Aims and methods in non-isothermal reaction kinetics. *J. Anal. Appl. Pyrolysis* **2007**, *79*, 278-288.

24.   Várhegyi, G.; Sebestyén, Z.; Czégény, Z.; Lezsovits, F.; Könczöl, S. Combustion kinetics of biomass materials in the kinetic regime. *Energy Fuels* **2012**, *26*, 1323-1335.

25.   Várhegyi, G.; Chen, H.; Godoy, S. Thermal decomposition of wheat, oat, barley and *Brassica carinata* straws. A kinetic study. *Energy Fuels* **2009**, *23*, 646-652.

26. Várhegyi, G.; Szabó, P.; Mok, W. S. L.; Antal, M. J., Jr. Kinetics of the thermal decomposition of cellulose in sealed vessels at elevated pressures. Effects of the presence of water on the reaction mechanism. *J. Anal. Appl. Pyrolysis* **1993**, *26*, 159-174.

27. DeGroot, W. F.; Pan, W.-P.; Rahman, M. D.; Richards, G. N. First chemical events in pyrolysis of wood. J. Anal. Appl. Pyrolysis, **1988**, *13*, 221-231.

28. Várhegyi, G.; Antal, M. J.; Jr.; Jakab, E.; Szabó, P. Kinetic modeling of biomass pyrolysis. *J. Anal. Appl. Pyrolysis* **1997**, *42*, 73-87.

29. Várhegyi, G.; Antal, M. J., Jr.; Székely, T.; Till, F.; Jakab, E. Simultaneous thermogravimetric – mass spectrometric studies on the thermal decomposition of biopolymers. Part 1: Avicel cellulose in the presence and absence of catalysts. *Energy Fuels* **1988**, *2*, 267-272.

30. Antal, M. J., Jr.; Várhegyi, G. Cellulose pyrolysis kinetics: The current state of knowledge. *Ind. Eng. Chem. Res.* **1995**, *34*, 703-717.

31. Várhegyi, G.; Szabó, P.; Jakab, E.; Till, F.; Richard J-R. Mathematical modeling of char reactivity in Ar-O_2 and CO_2-O_2 mixtures. *Energy Fuels* **1996**, *10*, 1208-1214.

32. Wang, L.; Várhegyi, G.; Skreiberg, Ø.; Li, T.; Grønli, M.; Antal, M. J. Combustion characteristics of biomass charcoals produced at different carbonization conditions. A kinetic study. *Energy Fuels* **2016**, *30*, 3186-3197.

33. Grønli, M.; Antal, M. J., Jr.; Várhegyi, G. A round-robin study of cellulose pyrolysis kinetics by thermogravimetry. *Ind. Eng. Chem. Res.* **1999**, *38*, 2238-2244.

34. Várhegyi, G.; Antal, M. J., Jr.; Székely, T.; Szabó, P. Kinetics of the thermal decomposition of cellulose, hemicellulose and sugar cane bagasse. *Energy Fuels* **1989**, *3*, 329-335.

35.   Raveendran, K.; Ganesh, A.; Khilar, K. C. Pyrolysis characteristics of biomass and biomass components. *Fuel* **1996**, *75*, 987-998

36.   Jakab, E.; Faix, O.; Till, F.; Székely, T. Thermogravimetry/mass spectrometry study of six lignins within the scope of an international round robin test. J. Anal. Appl. Pyrolysis 1995, 35, 167-179.

37.   Jakab, E.; Faix, O.; Till, F. Thermal decomposition of milled wood lignins studied by thermogravimetry/mass spectrometry. J. Anal. Appl. Pyrolysis 1997, 40-41, 171-186.